

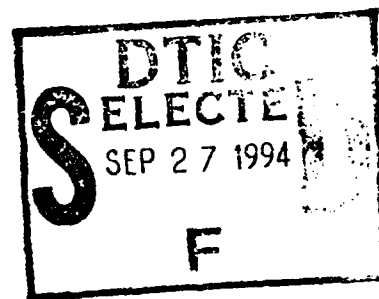
AD-A284 906



A TRIDENT SCHOLAR PROJECT REPORT

NO. 214

"THE EFFECTS OF PRIOR PITTING DAMAGE
ON REPASSIVATION POTENTIAL"



11412
94-30769



UNITED STATES NAVAL ACADEMY
ANNAPOLIS, MARYLAND

This document has been approved for public
release and sale; its distribution is unlimited.

94 9 26 097


U.S.N.A. - Trident Scholar project report; no. 214 (1994)

**"THE EFFECTS OF PRIOR PITTING DAMAGE
ON REPASSIVATION POTENTIAL"**

by
Midshipman Jason R. Frei, Class of 1994
U.S. Naval Academy
Annapolis, Maryland


Adviser: Assoc. Prof. Patrick J. Moran
Department of Mechanical Engineering

Accepted for Trident Scholar Committee


Chair


Date

Accession For	
NTIS CRA&I	<input checked="checked" type="checkbox"/>
DTIC TAB	<input type="checkbox"/>
Unannounced	<input type="checkbox"/>
Justification _____	
By _____	
Distribution/ _____	
Availability (C) _____	
Dist	Avail and Special
A-1	

DTIC QUALITY INSPECTED 3

REPORT DOCUMENTATION PAGE			Form Approved OMB no. 0704-0188	
<small>Public reporting burden for this collection of information is estimated to average 1 hour of response, including the time for reviewing instructions, searching existing data sources, gathering and maintaining the data needed, and completing and reviewing the collection of information. Send comments regarding this burden estimate or any other aspect of this collection of information, including suggestions for reducing this burden, to Washington Headquarters Services, Directorate for Information Operations and Reports, 1215 Jefferson Davis Highway, Suite 1204, Arlington, VA 22202-4302, and to the Office of Management and Budget, Paperwork Reduction Project (0704-0188), Washington DC 20503.</small>				
1. AGENCY USE ONLY (Leave blank)		2. REPORT DATE 19 May 1994		3. REPORT TYPE AND DATES COVERED
4. TITLE AND SUBTITLE The effects of prior pitting damage on repassivation potential				5. FUNDING NUMBERS
6. AUTHOR(S) Jason R. Frei				
7. PERFORMING ORGANIZATIONS NAME(S) AND ADDRESS(ES) U.S. Naval Academy, Annapolis, MD				8. PERFORMING ORGANIZATION REPORT NUMBER USNA Trident Scholar project report; no. 214 (1994)
9. SPONSORING/MONITORING AGENCY NAME(S) AND ADDRESS(ES)				10. SPONSORING/MONITORING AGENCY REPORT NUMBER
11. SUPPLEMENTARY NOTES Accepted by the U.S. Trident Scholar Committee				
12a. DISTRIBUTION/AVAILABILITY STATEMENT This document has been approved for public release; its distribution is UNLIMITED.				12b. DISTRIBUTION CODE
13. ABSTRACT (Maximum 200 words) There has been considerable controversy over the relationship between repassivation potential and pit size in passive metals such as aluminum and stainless steel. Understanding this behavior is very important when determining the appropriate level of cathodic protection for previously damaged systems. The repassivation-size relationship was explored in this experiment using a procedure known as the Scanning Reference Electrode Technique or SRET. Steel and aluminum samples were immersed in a 3.5 wt% NaCl solution simulating sea water. The samples were then polarized above the pitting potential and pitting activity was measured on a pit by pit basis with the SRET. The potential was then lowered in 0.1 V steps until all pits repassivated. No data was obtained for the aluminum due to its pitting characteristics, however, data was collected and analyzed on an individual pit basis for the 316 stainless steel. The pits analyzed varied in diameter from 0.31 mm to 1.63 mm, and showed repassivation potentials between 0.6 V and 0.5 V (vs. SCE). The data showed a decrease in repassivation potential of 0.093 V for an increase in diameter of 1 mm. This demonstrates that when cathodically protecting a damaged system, the level of protection must be held below the repassivation potential of the largest pit.				
14. SUBJECT TERMS corrosion, pitting, repassivation potential, prior damage, stainless steel				15. NUMBER OF PAGES
				16. PRICE CODE
17. SECURITY CLASSIFICATION OF REPORT UNCLASSIFIED		18. SECURITY CLASSIFICATION OF THIS PAGE UNCLASSIFIED		19. SECURITY CLASSIFICATION OF ABSTRACT UNCLASSIFIED
				20. LIMITATION OF ABSTRACT UNCLASSIFIED

ABSTRACT

There has been considerable controversy over the relationship between repassivation potential and pit size in passive metals such as aluminum and stainless steel. Understanding this behavior is very important when determining the appropriate level of cathodic protection for previously damaged systems. The repassivation-size relationship was explored in this experiment using a procedure known as the Scanning Reference Electrode Technique or SRET. Steel and aluminum samples were immersed in a 3.5 wt% NaCl solution simulating sea water. The samples were then polarized above the pitting potential and pitting activity was measured on a pit by pit basis with the SRET. The potential was then lowered in 0.1 V steps until all pits repassivated.

No data was obtained for the aluminum due to its pitting characteristics, however, data was collected and analyzed on an individual pit basis for the 316 stainless steel. The pits analyzed varied in diameter from 0.31 mm to 1.63 mm, and showed repassivation potentials between 0.6 V and 0.5 V (vs. SCE). The data showed a decrease in repassivation potential of 0.093 V for an increase in diameter of 1 mm. This demonstrates that when cathodically protecting a damaged system, the level of protection must be held below the repassivation potential of the largest pit.

KEY WORDS: corrosion, pitting, repassivation potential, prior damage, stainless steel

TABLE OF CONTENTS

ABSTRACT.....	1
INTRODUCTION AND OBJECTIVES.....	4
BACKGROUND.....	6
PROCEDURE.....	25
RESULTS AND DISCUSSION.....	38
CONCLUSIONS.....	46
ACKNOWLEDGEMENTS.....	48
REFERENCES.....	49

LIST OF FIGURES

FIGURE 1:.....	8
FIGURE 2:.....	10
FIGURE 3:.....	12
FIGURE 4:.....	15
FIGURE 5:.....	17
FIGURE 6:.....	19
FIGURE 7a:.....	22
FIGURE 7b:.....	22
FIGURE 8:.....	28
FIGURE 9a:.....	30
FIGURE 9b:.....	30
FIGURE 10:.....	35
FIGURE 11:.....	36
FIGURE 12:.....	41
FIGURE 13:.....	44

LIST OF TABLES

TABLE 1.....	26
TALBE 2.....	40
TABLE 3.....	40
TABLE 4.....	43

INTRODUCTION AND OBJECTIVES

The marine operating environment of the United States Navy places great demands on the materials used to construct our ships and aircraft. The poor corrosion performance of many metals in this environment has forced the Navy, over the years, to move toward more corrosion resistant materials for key applications such as turbines and weaponry components. While in numerous cases the use of these materials have greatly reduced uniform corrosion damage, many are still susceptible to pitting attack. Because of its common occurrence and damaging effects, pitting corrosion has been the subject of a large number of studies over the past three decades [1]. While scientists and engineers have made great steps toward understanding the causes of pitting and controlling its initiation and growth, many key aspects of the process itself are still not fully understood.

One area of ongoing speculation is the relationship between prior pitting damage and the repassivation potential of a material. Prior studies in this area have produced contradictory results [2,3,4,5]. One of the difficulties in studying this relationship has been acquiring in situ-data for individual pits. Single pits have been obtained in constant potential experiments by mechanically damaging the surface of a material or using small electrodes. However, these methods have not employed in-situ observation of the repassivation

process. One possible solution to this problem is called the Scanning Reference Electrode Technique (SRET), has shown promise in providing this type of data on a pit-by-pit basis.

The objectives of this project were twofold. The first was to determine the relationship between prior pitting damage and repassivation potential in 316 stainless steel and 6061-T6 aluminum on a pit-by-pit basis. The second objective was to evaluate the effectiveness of the Scanning Reference Electrode Technique in acquiring in-situ data for these materials.

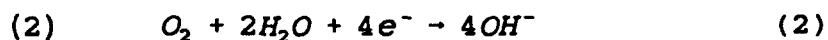
BACKGROUND

Ores are mined and then refined into a pure metal which can then be combined with other elements to produce an alloy. This refining process requires large amounts of energy to push the metals out of their thermodynamically stable natural state. A good example of this is the refinement of aluminum. Corrosion occurs because of the tendency of materials to spontaneously revert from this refined state back to a more stable natural form similar to and sometimes identical to the original ore [1]. A clear example of this behavior occurs when iron oxide ore is refined into iron which can then be processed into steel. The rust seen on steel is in fact iron oxide. Thus in corroding, the iron in the steel reverts back to its natural state. This basic corrosion reaction is an oxidation or anodic dissolution reaction and can be generalized as shown in equation 1.



Three key elements are necessary for this oxidation reaction to occur. First, there must be an aggressive environment, usually containing oxygen, which allows the metal M^{n+} ions to be carried into the bulk solution. There must also be a cathodic reaction, usually oxygen reduction in a seawater environment, which is shown in equation 2.

This cathodic reaction absorbs the electrons generated at the



anode. Finally, there must be a conductive path between the anode and the cathode to carry the electrons and the ions generated in the reaction. When these three conditions are met, the corrosion of metals is possible.

The driving force for the corrosion of metals is the difference in electrochemical potential (E) between the anodic reaction and the cathodic reaction. The greater the difference between the cathodic and anodic potential, the more likely and rapid the corrosion reaction. This difference between cathodic and anodic potentials is known as E_{cell} and is shown in equation 3.

$$E_{cell} = E_{cathode} - E_{anode} \quad (3)$$

The most common form of corrosion is uniform corrosion, which attacks the entire surface of a metal and corrodes it at a uniform rate [1]. Examples of this type of corrosion are the rusting of iron or the tarnishing of silver. Metals that suffer from this form of corrosion are known as active metals. Active metals typically show a logarithmic increase in the current density, with a linear increase in potential. Current density, found by dividing the total current from a corrosion reaction by the surface area of the metal, is proportional to the corrosion rate. This behavior is shown in Figure 1 in what is known as a polarization curve [1]. The anodic

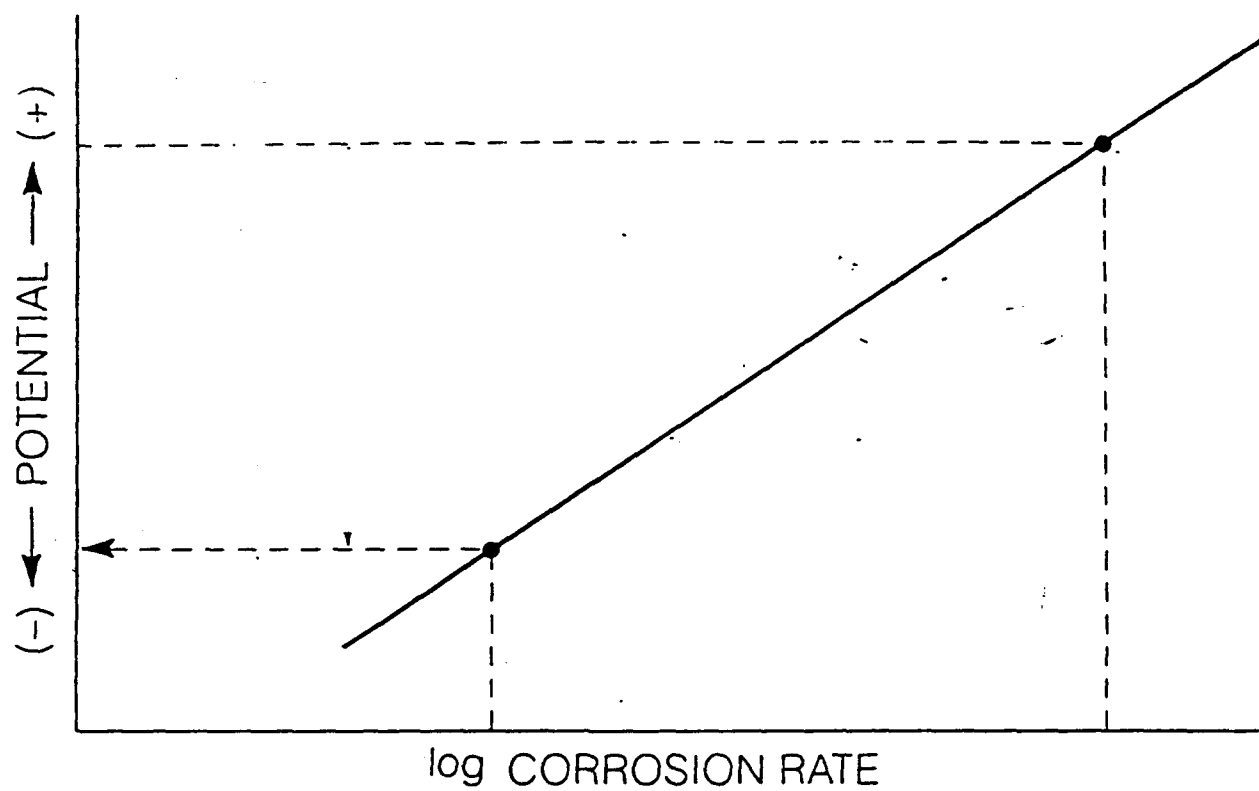


FIGURE 1: Polarization curve for an active metal.

potential achieved by a metal depends on the potential of the particular cathodic reaction in the service environment.

Fortunately, not all metals are subject to uniform corrosion in a seawater environment. The initial uniform corrosion products of many materials, such as aluminum, stainless steel, and titanium, are oxides that form a thin protective film over the surface of the metal. This film isolates the substrate metal from the aggressive environment and prevents further uniform corrosion. Metals capable of forming these protective oxide films are known as passive metals [1]. At low potentials, these passive materials show a logarithmic increase in current density with increasing potential. This voltage range is known as the active region of the polarization curve shown in Figure 2 [1]. At a potential known as the passivation potential (E_{pp}), the passive metal will form an oxide film, stopping uniform corrosion and dropping the current density to a much lower level (i_{pass}). This passive oxide film is only protective, however, within a certain potential range. The upper limit of this passive region is known as the pitting potential (E_{pit}). Once the potential is raised above E_{pit} , the metal enters the transpassive range and undergoes pitting corrosion. The mechanism leading to the initiation of pitting corrosion is not completely understood and is beyond the scope of this Trident Scholar Project [7]. It is known, however, that pitting occurs in two phases: initiation and propagation.

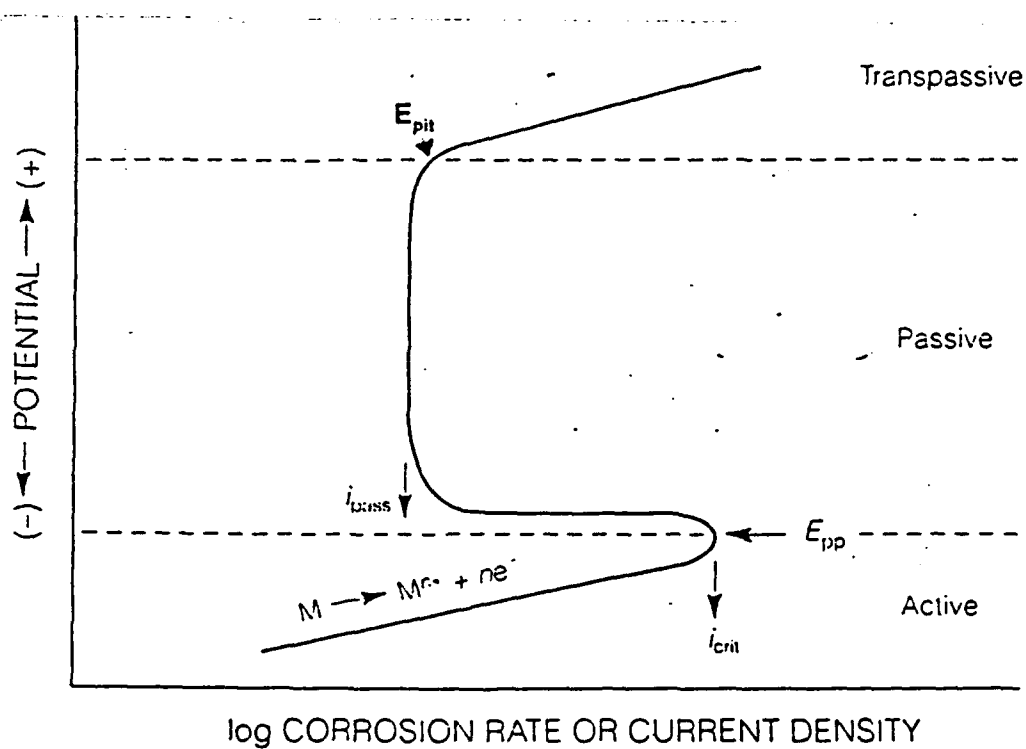


FIGURE 2: Polarization curve for an passive metal.

During the initiation phase, the metal surface suffers little or no damage as pits undergo an incubation period which involves the deterioration of the passive film at discrete sites. When the pits enter the propagation phase, these discrete sites propagate or grow and new sites continue to develop [8]. During this propagation phase, small increases in potential yield very large increases in current density, which is a measure of the corrosion rate.

Large increases in current are much more damaging for pitting corrosion than for uniform corrosion. While uniform corrosion removes metal over the entire surface of a material, pitting acts at discrete sites, corroding the metal in a very small area. The removal of metal from these small surface areas can cause the pits to extend deep into the substrate metal. These deep pits can then develop a solution chemistry much more aggressive (very low pH due to metal hydrolysis) than the bulk solution [9]. The larger the pit grows, the more occluded the local environment becomes and the more aggressive the attack. In addition, the environment can have a large effect on the corrosion rate. One environmental factor is the concentration of chloride anions, which are present in a seawater environment. While the exact role of the Cl^- is not completely understood, it has been shown that these ions greatly accelerate pitting [7,9]. Because of the aggressive nature of pitting, the major consideration when using passive materials is to ensure that they remain in their

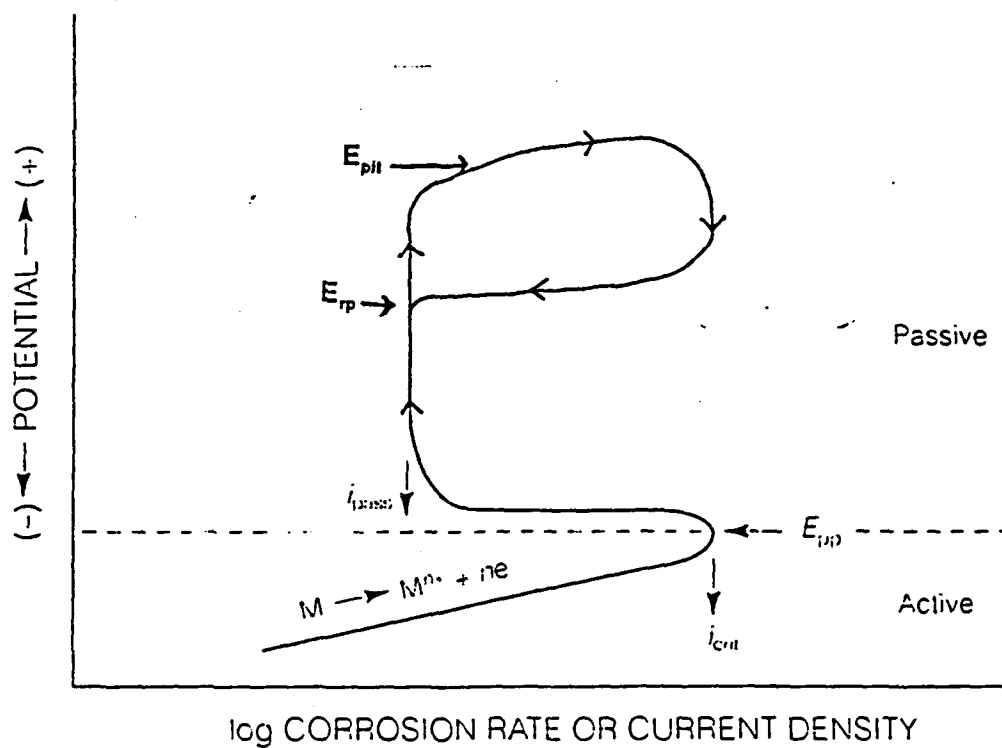


FIGURE 3: Polarization curve for a passive metal showing repassivation behavior.

passive range.

Finding the polarization behavior of a passive material and the potential at which passivity breaks down is complicated by several factors. Figure 3 shows a more complete polarization curve than the one presented in Figure 2. As can be seen in Figure 3, if the potential is raised out of the passive range and then reversed, or moved back in the negative direction, the data typically do not retrace the initial potential-current-density curve. Instead, the data will trace a new curve as the potential is reduced to a level below the original E_{pit} . This reduction of potential allows the pits to regenerate their protective oxide film, causing the current-density to approach the original i_{pass} . However, this occurs at a potential which is lower than the original E_{pit} . This process is known as repassivation and the potential at which it occurs is called the repassivation potential (E_{rp}).

There has been considerable controversy over whether E_{pit} and E_{rp} are reproducible and thereby truly representative of a material. These potentials have been shown to depend on several factors including the rate at which the potential was increased and the amount of damage allowed to develop on the specimens before the potential scan was reversed. Some authors have even argued that there is no fundamental difference between the passivation and repassivation potentials if the repassivation potential is measured after allowing very minimal pitting [4,10].

Much of the interest in the behavior of the repassivation and pitting potentials lies on the mechanistic level. However, these potentials also have great practical importance as key information for a widely used corrosion prevention system known as cathodic protection. Figure 4 shows a schematic diagram of an example of metal M dissolution, liberating a metal ion M^{2+} into solution and electrons, e^- , which are then consumed in the aqueous reduction of O_2 to OH^- . The electrochemical reaction shown in Figure 4 is limited by the mobility of the O_2 molecules in solution. If electrons are made available at the metal surface by applying a current to the system, the potential at the surface becomes more negative slowing down or possibly stopping the corrosion reaction. The application of current in this manner is known as cathodic protection. Therefore, by controlling the magnitude of the applied current with a cathodic protection system, the potential of the system and the rate of corrosion can be regulated.

When using a cathodic protection system on a passive metal, the potential is held in the passive range below E_{pit} and above E_{pp} . While this type of protection is sufficient for undamaged materials, complications occur when a cathodic system is used to protect metals that have already experienced some attack. With prior damage, it is necessary to hold the potential of a system below the E_{rp} to prevent prior pits from activating. It has been qualitatively shown [4,5,6], however,

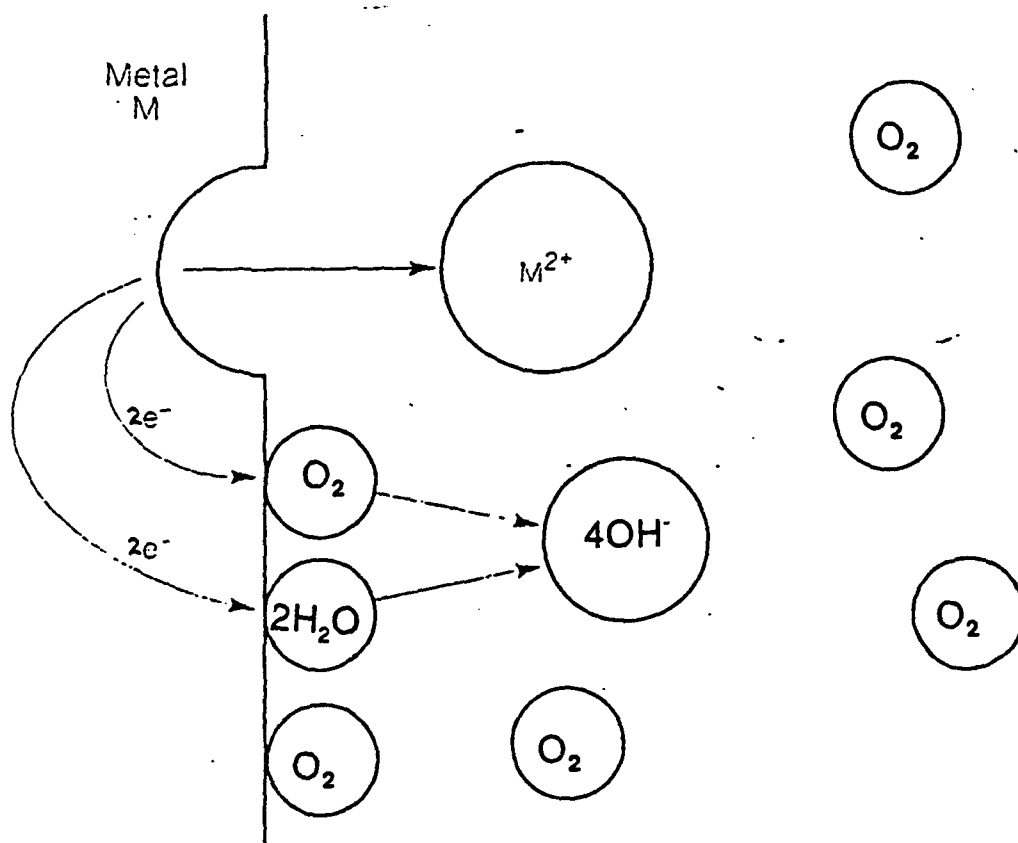


FIGURE 4: Schematic diagram of metal M dissolution.

that the magnitude of E_{rp} is a function of the amount of prior pitting attack. Thus, in order to determine the potential required to cathodically protect a previously pitted system, the relationship between E_{rp} and prior pitting damage must be determined.

One of the first studies to recognize the relationship between repassivation potential and prior damage was done in 1972 by B.E. Wilde [5]. One of the findings of this study was the fact that pits initiated at potentials above E_{pit} would continue to grow when the potential was dropped to a value between E_{pit} and E_{rp} . To examine this behavior, Wilde generated several polarization curves as shown in Figure 5 for Type 430 stainless steel (C .12 max, Cr 16.00-18.00, Mn 1.00 max, P 0.040 max, S 0.030 max, Si 1.00 max) in a 1M NaCl solution [11]. In each successive curve, Wilde allowed pits to propagate to higher current densities which correspond to greater amounts of pitting. The higher the current density allowed, the more extensive the pitting damage on the specimen. As his results show, if more damage was allowed to develop (i.e. the current density was raised to a higher level) prior to shifting the potential scan in the negative direction, the pits continued to propagate at successively lower potentials. Thus, according to Wilde's study, the repassivation potential is inversely related to prior pitting damage.

This relationship between E_{rp} and prior damage was called

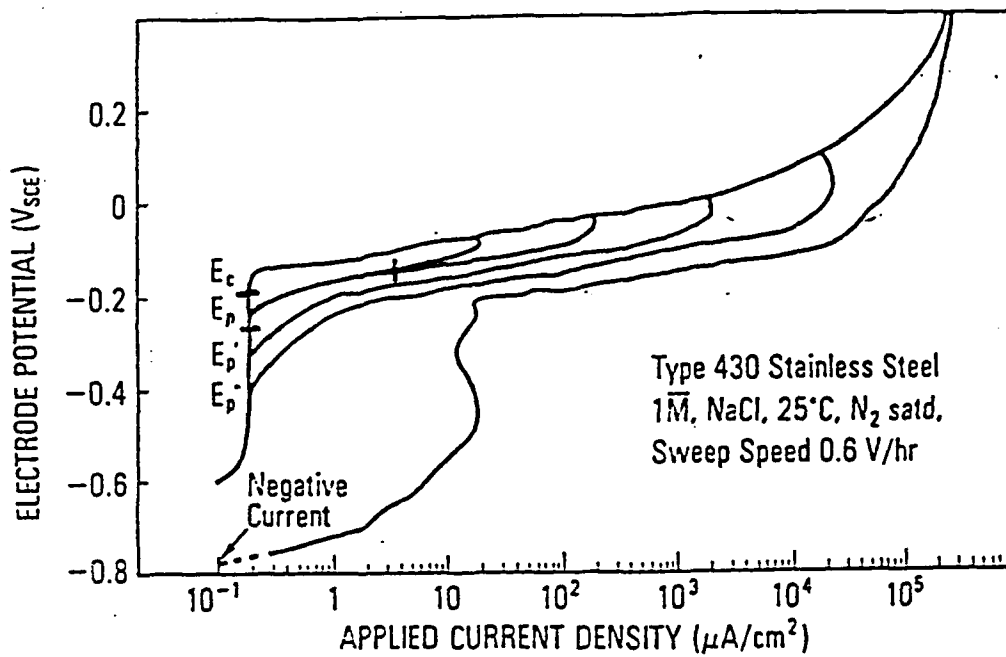


FIGURE 5: Wilde study polarization curves.
($E_c = E_{pit}$, $E_p = E_{rp}$)

into question by a study done in 1984 by R.C. Newman and E.M.Franz on AISI 304 stainless steel (C 0.08 max, Cr 18.00-20.00, Mn 2.00 max, Ni 8.00-12.00, P 0.045 max, S 0.030 max, Si 1.00 max) in a 1 M NaCl solution [2]. While Wilde's study involved multiple pits spread over the surface of a sample, Newman and Franz allowed only a single pit to grow on a fairly small specimen. Therefore, the repassivation potential measured in the experiment could be directly correlated to a specific pit, allowing the actual physical size of the pit to be measured. This was done both with a stereoptic microscope and by measuring the total electrochemical charge passed during pit growth, designated as Q . The amount of metal lost from the pit could then be calculated from the electrochemical charge. The relationship between total charge and pit radius was found to be

$$r \propto Q^{\frac{1}{3}} \quad (4)$$

assuming the pits were hemispherical in shape. In the experiment, a single pit was allowed to initiate and grow to a desired size. The potential was then scanned downward until the pit repassivated. The repassivation potentials (in this study abbreviated as E_p), pit depth parameter $Q^{1/3}$, and radius from numerous runs are compared in Figure 6 [2]. This figure shows that the repassivation potential remains fairly constant as pit size increases. Although several pits do show lower

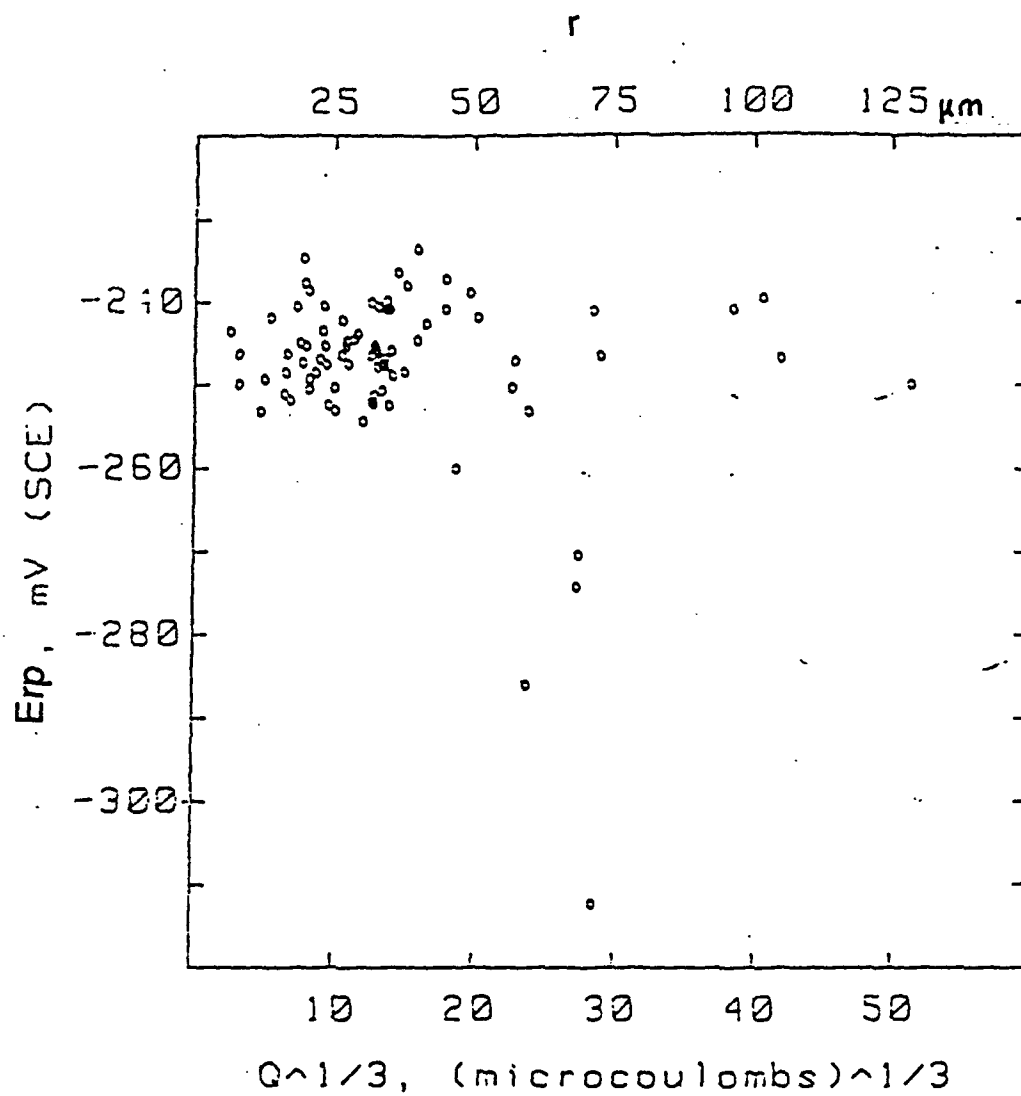


FIGURE 6: Newman and Franz plot of repassivation potential vs. pit size.

potentials for increasing size, Newman felt that this is due to the "unusual occluded geometries" of these pits. Because of this unusual geometry, Newman felt that these data were not representative of the actual E_{rp} , prior damage relationship.

According to Newman and Franz, unusually occluded pits were responsible for the inverse relationship between E_{rp} and the amount of attack in the Wilde study. Newman and Franz asserted that Wilde's inverse relationship was primarily caused by a variation in the number of pits in the experiment. When many pits were initiated on a specimen, there was a higher probability that one of them would have an "unusual occluded geometry" and not repassivate. These pits would repassivate at a lower potential which was not representative of the actual behavior of the pits on the specimen. They proposed that when the values from these pits were excluded, the data would show that E_{rp} was independent of pit size. Therefore, according to Newman and Franz, the repassivation potential of a pit is not a function of the prior damage.

The Newman study was revolutionary in that it was the only major study to look at the repassivation characteristics of a material on a single pit basis. The individual pit approach is unquestionably superior in determining the actual behavior of pits in a metal. However, in order to propagate only single pits, Newman was forced to alter the service environment of his experiment by adding 0.04 M sodium

thiosulfate ($\text{Na}_2\text{S}_2\text{O}_3$) to his solutions. This calls into question whether or not the results of Newman's study are actually characteristic of the metal or are a result of the altered environment. In addition, Newman discounts the data from the "unusually occluded" pits. However, in an actual corrosion environment, this type of pit will be present and thus its behavior and macroscopic effects must be taken into consideration.

A third study, conducted in 1992 by N.G. Thompson and B.C. Syrett, examined the E_{pit} and E_{rp} parameters of alloy G3 (C 0.015 max, Co 5.0 max, Cr 21.0-23.5, Cu 1.5-2.5, Fe 18.0-21.0, Mn 1.0 max, Mo 6.0-8.0 Ni rem) [11] and 317 stainless steel (C 0.08 max, Cr 18.00-20.00, Mn 2.00 max, Mo 3.00-4.00, Ni 11.00-15.00, P 0.045 max, S 0.030 max, Si 1.00 max) [11] in solutions containing high levels of Cl^- [4]. In this study, the potential of specimens was polarized above E_{pit} to allow the onset of pitting. After a predetermined time, the applied potential was moved to a more negative value and the current measured for another set period. This was then repeated, with the potential being gradually lowered in small steps, until total current levels from the specimen indicated that all the pits had repassivated. The measure of pit damage in these experiments was the length time between initiation and repassivation for the specimen. The longer the specimen was actively pitting, the greater the pit damage.

The results of these experiments are shown in Figures 7a

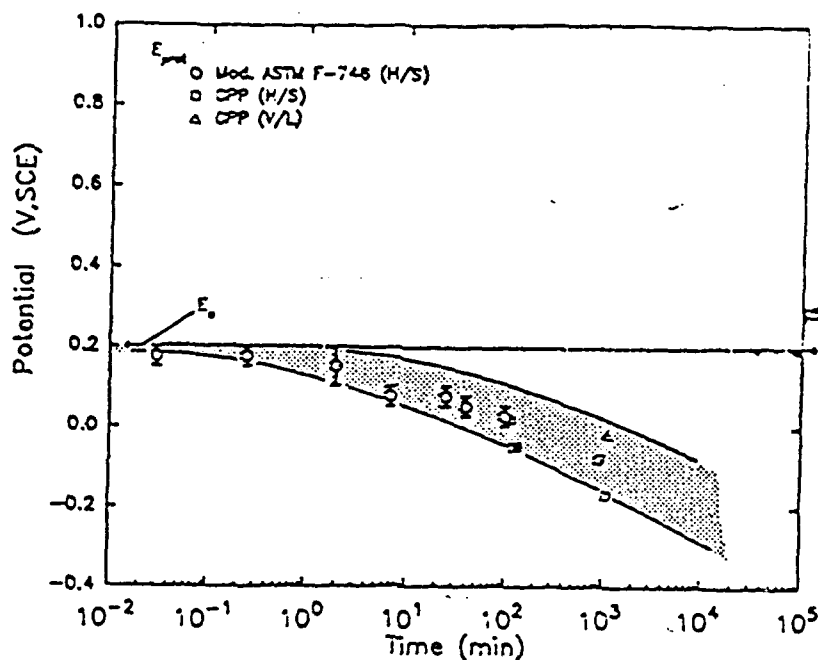


FIGURE 7a: Thompson and Syrett plot of potential vs. Time relationship for E_{pit} and E_{rp} for type 3171 SS.

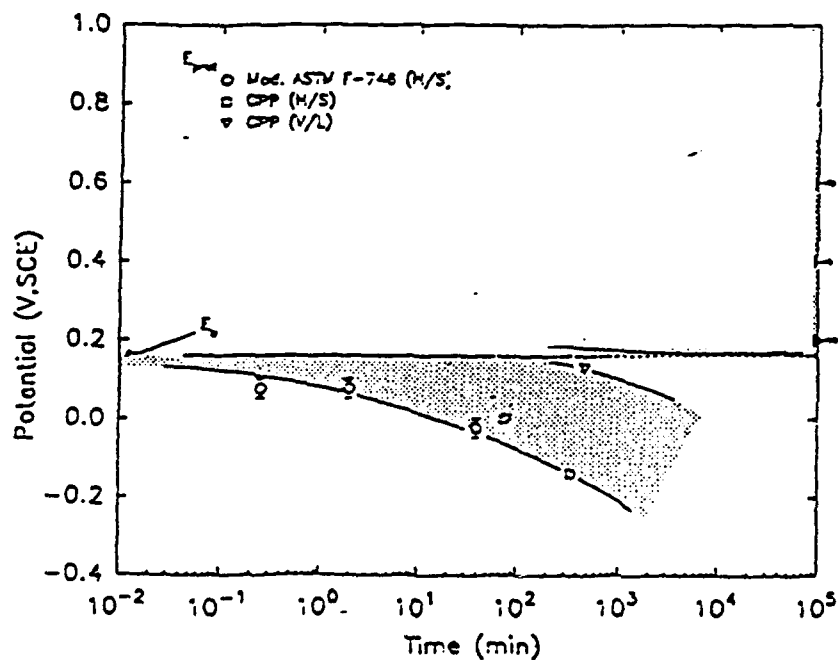


FIGURE 7b: Thompson and Syrett plot of potential vs. Time relationship for E_{pit} and E_{rp} for Alloy G3.

and 7b. Although there is significant scatter in the data for both alloys, both plots show a decrease in the pitting potential as time (or pit damage) increases. Therefore, this Thompson-Syrett study shows an inverse relationship between prior damage and repassivation potential. This is consistent with the conclusion of the Wilde study.

These three studies, along with numerous others, indicate the continuing controversy concerning E_{rp} and pit damage. The objective of this Trident Research Project was to resolve the relationship between repassivation potential and prior pitting damage. To do this, the single pit approach was selected to allow a direct comparison between repassivation potential and actual pit size. It was also decided that altering the environment by adding chemicals to allow single pit propagation was undesirable, as these chemicals are rarely found in a service environment. To acquire this single pit data in an unaltered environment, a new system developed by EG&G Applied Research and the Royal Naval Engineering College in Plymouth, England, was used. This system is known as the Scanning Reference Electrode Technique or SRET.

The SRET collects data with a probe consisting of two small wires that measure the voltages caused by current in solution close (approximately 1 mm) to the surface of a specimen. An actively corroding area on the metal surface creates a voltage field gradient in the solution around the pit as ions and current move outward from the anodic pit into

the solution. The more active the pit, the more intense the field. By measuring this voltage, the SRET can determine the amount of corrosion occurring at very discrete sites on the surface of a specimen. As this data is collected, the cylindrical specimen in the SRET rotates, allowing the probe to generate a line of discrete voltage measurements from the specimen's circumference. After one revolution, the probe is lowered to a new line and voltage data is taken for another thin band of the specimen. This scanning continues until the SRET has a complete set of voltage data for the area of interest on the cylindrical specimen. As the data are collected, the SRET stores the voltage values corresponding to current in solution to a digital 2-D map of the surface of the cylinder. The computer is then able to generate a color map of the current with respect to position on the specimen. With the SRET, the activity and size of a several specific pits in a multi-pit environment can be measured in-situ at any given time. This eliminates the complicated procedures needed to generate single pits and maintain a fairly realistic environment with multiple active sites for study.

PROCEDURE

AISI 316 stainless steel and 6061-T6 aluminum were obtained as 0.5 inch diameter round stock. The chemical composition of these materials is shown in Table 1 [11]. A 3-inch long specimen was cut and the mill scale removed by machining. The sides were then abraded to a 600 grit finish by spinning the specimen in a drill press and polishing with CarbiMet paper strips. The bottom of the specimen was polished by hand to the same finish. After washing with distilled water and air drying, the specimens were degreased with acetone. The prepared specimens were then inserted into the SRET and the electrical connection checked with a Fluke model 27 multimeter.

A 3.5 wt% NaCl solution, used to simulate seawater in the experiments, was made using 66.5 grams of NaCl measured on an Ohaus Dial-O-Gram balance. This was combined with 1,833 mL of distilled water in a 2 liter plastic bottle and agitated until all the salt was in solution. The glass solution bowl of the SRET was then filled with 1900 mL and a saturated calomel reference electrode (SCE) was inserted into this solution.

An EG&G Princeton Applied Research VersaStat potentiostat was connected to the specimen holder, the SCE, and the SRET's built-in graphite counter electrode. The SCE and graphite counter electrode were used to control the

TABLE 1			
METAL COMPOSITION			
wt% of Elements			
316 SS		6061-T6 Aluminum	
Element	wt %	Element	wt %
C	.08 max	Cr	.04-.35
Cr	16.0-18.0	Cu	.15-.40
Mn	2.00 max	Fe	.7 max
Mo	2.0-3.0	Mg	.8-1.2
Ni	10.0-14.0	Mn	.15 max
P	.045 max	Si	.40-.8
S	.030 max	Ti	.15 max
Si	1.00 max	Zn	.25 max
		Others	.05 max each
			.15 max total
Fe	Balance	Al	Balance

Chemical composition of AISI 316 Stainless Steel and 6061-T6 Aluminum.

electrochemical potential of the specimen. The specimen was then accelerated to a speed of 100 rpm and several line-scans were taken by the SRET to test the electronic noise in the system. The SRET was controlled with SRET Control and Analysis Software 1.31 which was installed on a 486 Everex Computer. If the line-scans did not indicate excessive noise in the system, a step-hold pattern (described below) was run with the potentiostat.

In the step-hold pattern, shown in Figure 8, the potential of the specimen was raised to a value well above the pitting potential of the metal. This was done with the PAR VersaStat, which was controlled by Model 352/252 Corrosion Analysis Software 2.01. Several area scans were made with the SRET at this potential to determine the amount of pit activity. When a sufficient range of pits had been established, the potential was lowered by 0.1 V and a potential map of the surface was again generated with the SRET. Each map generated by the SRET took approximately 20 minutes to generate. This process was repeated until all of the pits on the material had repassivated. The potential maps collected by the SRET were stored as digital maps on disk for further analysis.

6061-T6 ALUMINUM

The step-hold procedure was applied to the 6061-T6 aluminum, with the initial potential hold done at -0.6 V.

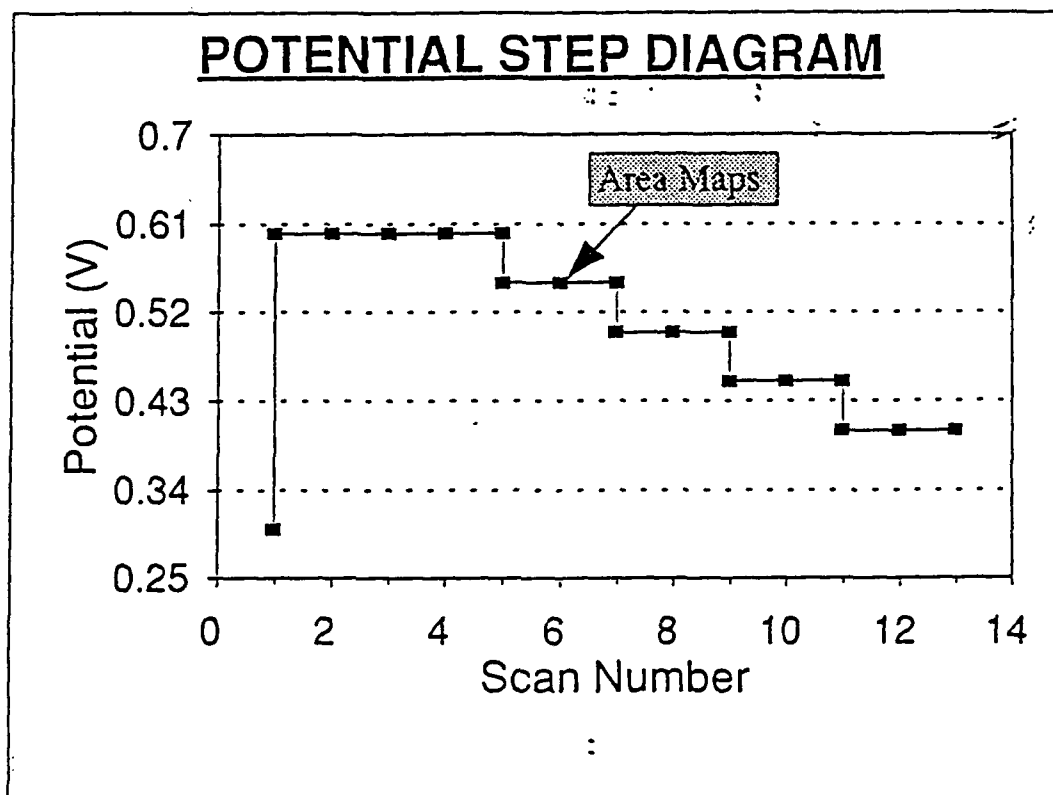


FIGURE 8: Step-hold pattern used for SRET data collection.

This potential was sufficient to cause the initiation and propagation of numerous pits over the entire surface of the material. The SRET, however, was not able to clearly map these pits. When the aluminum specimens were examined under the Scanning Electron Microscope after the experiment, the pits proved to be very shallow, with an average diameter of only 0.025 mm. Examples of this type of small pit are shown in Figures 9a and 9b. This small size indicated that the aluminum pits were only active for a short period of time and that they produced very low levels of current as they corroded. Because of this small level of current and the transient nature of the pitting, the SRET was not able to generate clear maps of the aluminum pits.

In an attempt to generate useful data from the aluminum specimens, a new preparation technique was tried. After the specimens were polished degreased with acetone, several indentations were made on the surface of the specimen using a diamond scratch. These indentations damaged the oxide film and therefore should have provided preferential pit initiation sites when the potential of the specimen was raised above E_{pit} . If these pits did initiate, their relatively large diameter of roughly 1 mm, would produce a large enough voltage field to be mapped by the SRET.

This new technique was tried in three experiments and was not successful. The pre-formed pits did begin to corrode when polarized above the pitting potential, but

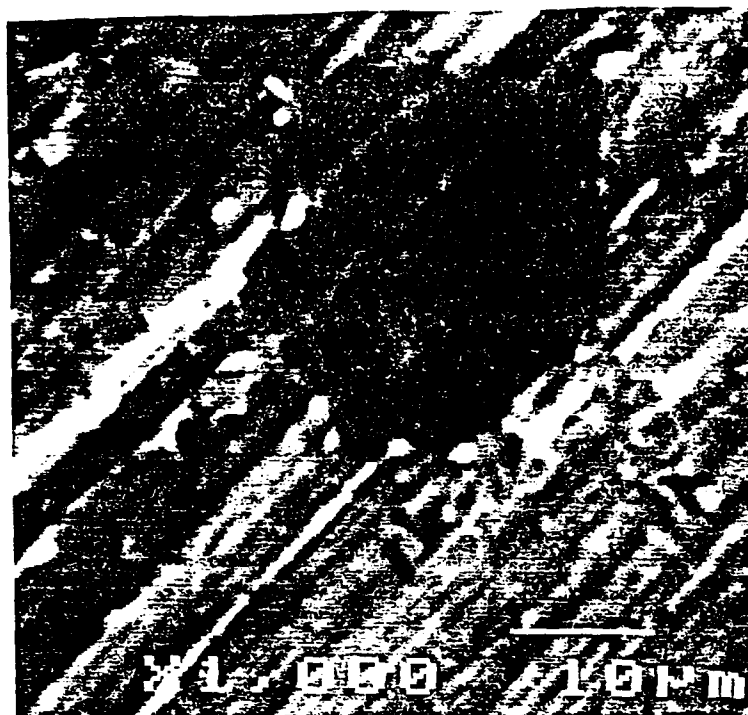




FIGURE 9a: SEM photo of a typical aluminum pit.
( = 10 μm)



FIGURE 9b: SEM photo of a typical aluminum pit.
( = 10 μm)

quickly repassivated. The small, shallow aluminum pits which then propagated were identical to those in the original experiments and could not be mapped. Because of this, no data could be collected for the 6061-T6 aluminum.

316 STAINLESS STEEL

The pits initiated in the 316 stainless steel with the step-hold technique were much larger than those in the aluminum specimens. When the potential was initially raised to 0.6 V, pits with diameters varying from 0.917 mm to 3.69 mm propagated on the stainless steel. In nearly all the experiments, a large number of these pits initiated on the bottom of the specimen. Because of their large size, the bottom pits used nearly all of the applied current and therefore, did not allow pitting on the sides of the specimen. Because the probe of the SRET was only able to map the sides, it was not possible to collect data when the specimen was subject to bottom attack. In addition, early in the project, specimens were also subject to water line crevice attack. The probe could not collect data from this area either, so no data was collected there.

The first attempt to control the bottom and water line attack on the specimens was to treat these areas with a 6 M solution of HNO_3 , which is a passivating acid for stainless steels. The HNO_3 prevented corrosion by thickening the protective oxide film of the stainless steel. To treat the

316 specimen, the specimen was inverted and the top lowered into a beaker with 300 mL of 6 M HNO_3 solution until the area that would be at the water line was submerged. The specimen was left in the acid bath for 30 minutes, removed, and rinsed with distilled water. Next, the bottom of the specimen was suspended in the HNO_3 solution for 30 minutes. The sample was then rinsed with distilled water and degreased with acetone. This treatment successfully eliminated the water line attack, however, it failed to stop the bottom pitting problem.

The next attempt at stopping the bottom attack was to pre-form pits with a diamond scratch on the sides of an acid treated specimen. These pre-formed pits did initiate when the potential was raised above E_{pit} in the experiment, but repassivated as the bottom pits began to propagate.

Another effort to prevent the bottom attack was to stop the rotation of the specimen while the pits initiated during the first potential hold at 0.6 V. It has been shown that the E_{pit} of a material is sensitive to the speed of rotation of a specimen [12]. Because the sides of the specimen are farther from the axis of rotation than any point on the bottom, the velocity at the sides is the maximum on the specimen. Thus, the pitting potential on the sides would be slightly higher than that of the bottom and therefore, the bottom would initiate first. This difference in E_{pit} proved to be insignificant at 100 rpm, however, with bottom attack

occurring both when the specimen was rotated or stopped.

The next method attempted to prevent bottom attack was to coat the bottom of the specimen with an epoxy. The West System Two Part Epoxy was used to coat the bottom and a small amount of the side of the specimen. After this dried, the edge of the epoxy was examined under a optical microscope to check the quality of the metal-epoxy bond. At x32 power, no gaps were visible between the 316 and the epoxy. When the specimen was raised above the pitting potential, severe crevice corrosion occurred at the edge of the epoxy. This crevice attack did not produce any mappable pits and protected the rest of the sides of the specimen in the same manner as the bottom attack.

After the West System epoxy, the next attempt to propagate pits on the sides was to round the bottom of the specimen. The bottom of the specimen was machined to a hemisphere with a diameter equal to that of the specimen. The rounded bottom was then polished to a 600 grit finish, rinsed, and degreased as before. The end of the specimen was rounded to alter any effects the geometry might have had on the current distribution on the specimen. When the rounded specimen was raised above E_{pit} , however, pits again initiated on the bottom, preventing data from being collected.

Another attempt to prevent bottom attack was to coat the rounded bottom of the specimen with an another epoxy: super-glue. This epoxy produces a tighter metal-epoxy bond and

therefore should have stopped the crevice attack seen with the West System. The super-glue coated specimen was polarized above the pitting potential to 0.5 V, and held for approximately 12 hours. After this period, no pitting was noticeable on the sides of the specimen, however, the entire bottom of the specimen had experienced severe corrosion damage. The epoxy coating on the bottom of the specimen had maintained its shape and acted as a cap, holding in the aggressive local solution. This aggressive solution had caused the severe bottom attack before the epoxy coating had fallen off of the specimen.

One possible reason for the bottom attack was a more aggressive solution chemistry underneath the specimen. This theory was tested by circulating solution over the bottom of the specimen during the initial potential hold for both rounded and flat-bottomed specimens. This method did not stop the bottom attack, and therefore, did not provide useful data.

Another possible explanation for the bottom pitting was grain boundary attack at the end grains on the bottom of the specimen. Scanning electron microscope analysis of the bottom of a 316 specimen showed large pits, partially covered with a thin layer of metal, as shown in Figure 10. This feature, along with the presence of grain facets in the corrosion pattern shown in Figure 11, suggested grain boundary attack. In order to stop this, the end of a specimen was fused using a welding torch

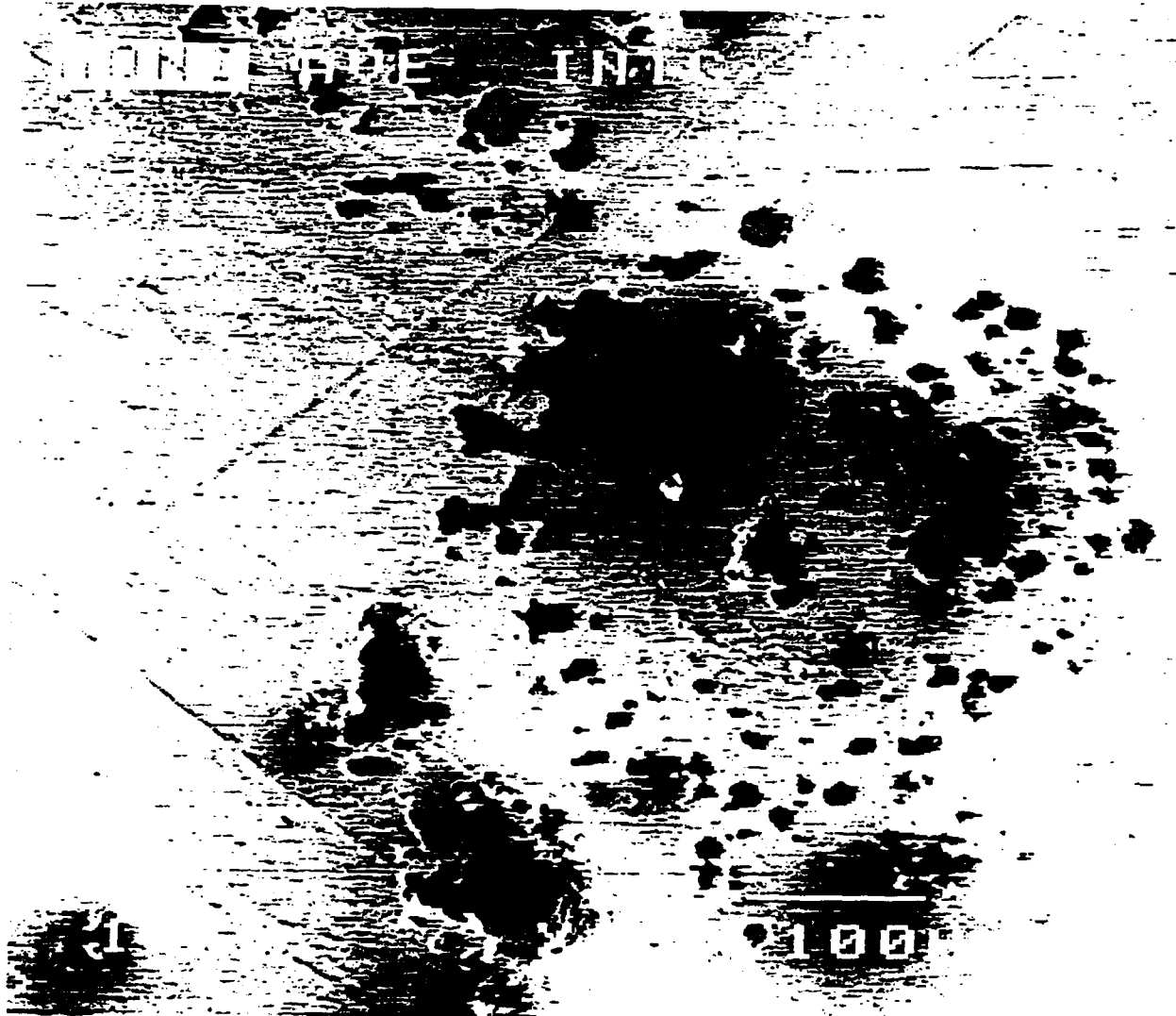


FIGURE 10: SEM photo of foil covered 316 stainless steel pit.
(\longleftrightarrow = 100 μm)

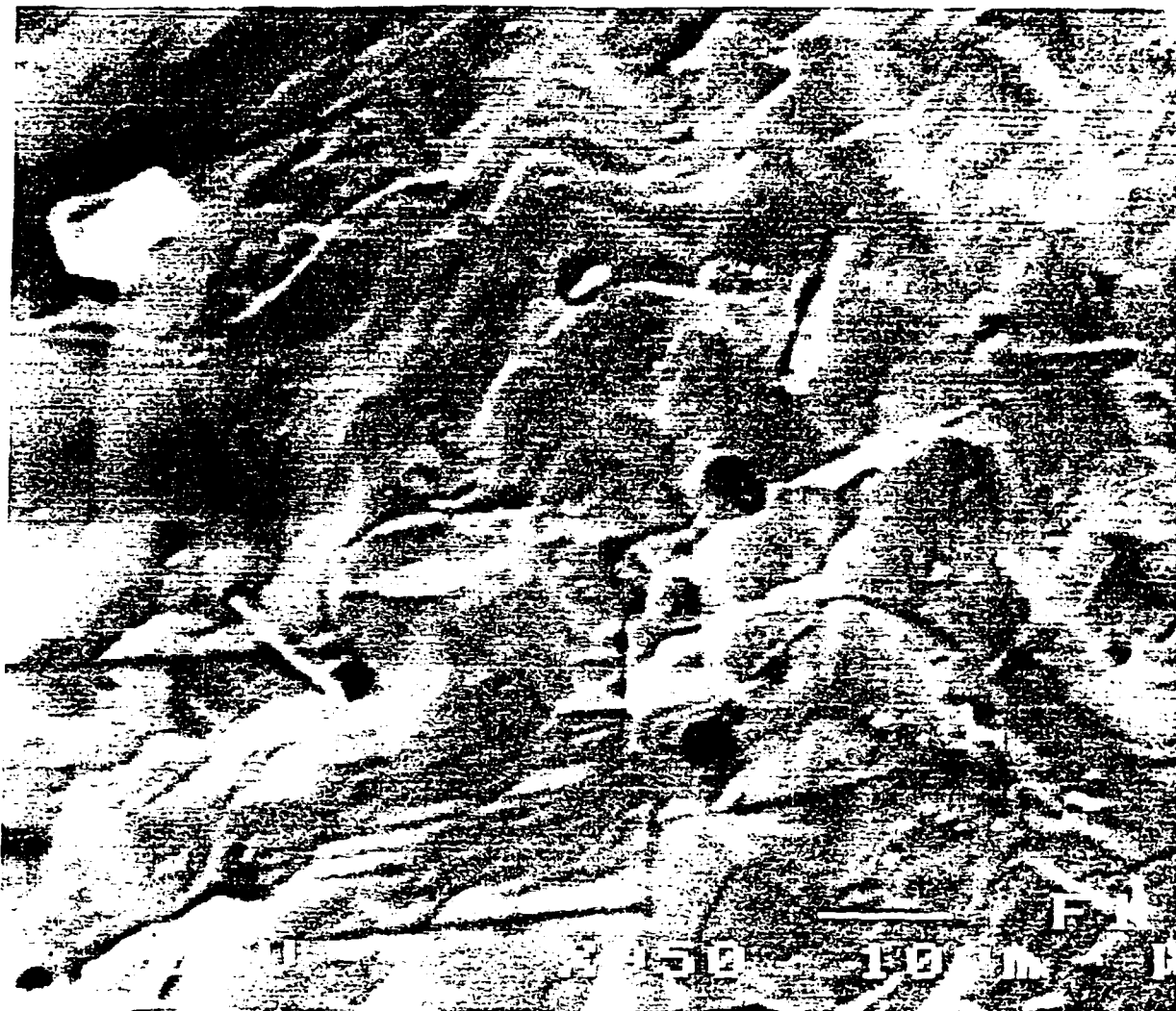


FIGURE 11: SEM photo of corrosion pattern inside a 316 stainless steel pit. ($\text{—} = 10 \mu\text{m}$)

in an attempt to reduce the number of grain boundaries. When this fused specimen was polarized above the pitting potential to 0.6 V, pits still preferentially initiated on the bottom and no pitting was detected on the sides of the specimen.

The final attempt to prevent the bottom attack was to isolate the bottom of the specimen from the solution with an inert gas. This was done by machining a hollow into the end of the specimen and filling this with N_2 . While the gas bubble covered most of the hollow, there was a small area that could not be covered. This area experienced severe pitting attack when the potential of the specimen was raised to 0.6 V and held for approximately 7 hours. Consequently, no pitting was detected on the sides of the specimen.

Of a total of 37 different experiments run on the 316 stainless steel, only 3 yielded appropriate data. It is not known why bottom attack did not occur in these experiments. The SRET maps generated in these runs were stored on computer disk and analyzed using the SRET Area Map Analysis Software, Version 1.21.

RESULTS AND DISCUSSION

The first step in analyzing the data was to determine the size of the pits on the area maps generated by the SRET. It is important to note that the values recorded by the SRET were potentials generated by the current passing in the solution. These potentials are representative of the pitting activity.

Using these area map potentials, a value of -2.0 mV was arbitrarily selected to define the edges of the pits on the maps. This value was input into the SRET Area Map Analysis Software, Version 1.21, which drew an equipotential line at -2.0 mV around each pit. The outlines of the pits generated by this method were all roughly circular. This pit geometry was confirmed by optical examination of the specimens. The agreement between the area maps and the actual pits observed with an optical microscope indicated that the pit outlines were representative of the actual shape of the pits. The next step in determining the map pit size was to find the highest level of activity for each pit in the series of maps generated in each experiment. It was assumed that the greatest amount of activity would occur as the pit reached its largest size. This damage would remain even after the level of activity decreased and the pit eventually repassivated. Thus, the highest level of activity on the maps would most closely approach the actual size of the pit. Once the most active map of a pit was found, the analysis program was used to measure the diameter of the pit in both the x and y direction. The x

and y diameters were then averaged. These values are displayed for each pit in Table 2.

The next step in the data analysis was to correlate the size of the pits on the area maps with the actual size of the pits on the specimen. To do this, each specimen was optically examined to locate the largest pit. The diameter of this pit was then physically measured and recorded. The series of area maps for the corresponding experiment were then examined to find the most active map of a pit. The most active pit map was assumed to be the largest pit on the specimen. The physical and map image diameters of the largest pit on each of the three specimens are shown in Table 3. A linear regression was then done on this data using Quattro-Pro, Version 1.0. This calculation indicated that the actual pits were .683 times smaller than the -2.0 mV outlines generated on the area maps. This value was used to convert the image diameters into physical diameters for the remaining pits using the calibration curve shown in Figure 12.

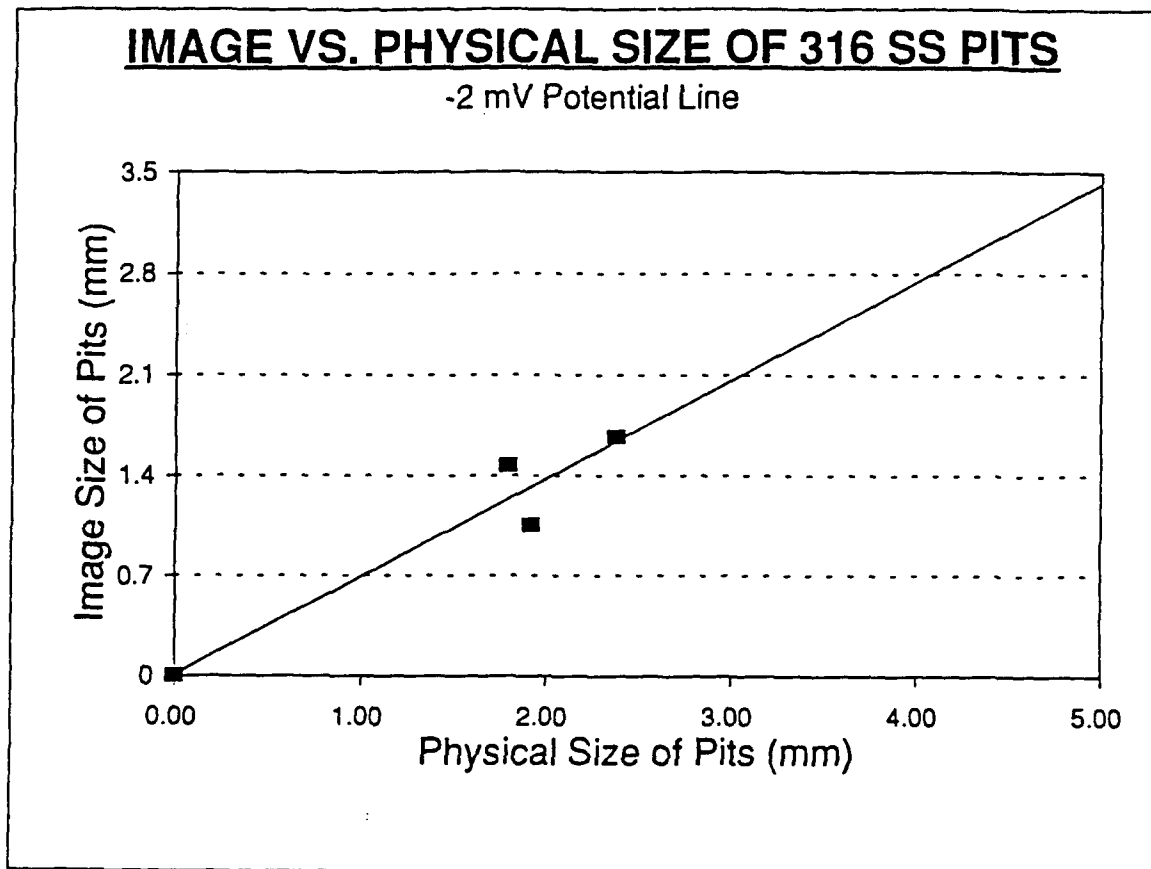
Once the physical diameters of the pits had been calculated, the repassivation potential for each pit in the experiment was found. When a pit repassivated during the

TABLE 2			
AREA MAP PIT DIAMETERS			
-2 mV Potential Outline			
Pit Number	X (mm)	Y (mm)	AVE (mm)
0	0.000	0.000	0.000
10	1.979	1.858	1.919
11	2.122	2.652	2.387
12	1.800	1.800	1.800

Measurements of pit diameters
from SRET Area Map Analysis.

TABLE 3		
PHYSICAL VS. MAP DIAMETERS		
-2 mV Potential Outline		
Pit Number	Map (mm)	Physical (mm)
10	1.919	1.055
11	2.387	1.671
12	1.800	1.470

Image and physical diameters
of largest pits in each
experiment



Regression Output:	
Constant	0.00615
Std Err of Y Est	0.24957
R Squared	0.92516
No. of Observations	4
Degrees of Freedom	2
X Coefficient(s)	0.68322
Std Err of Coef.	0.1374

FIGURE 12: Image size to physical size calibration curve for 316 stainless steel.

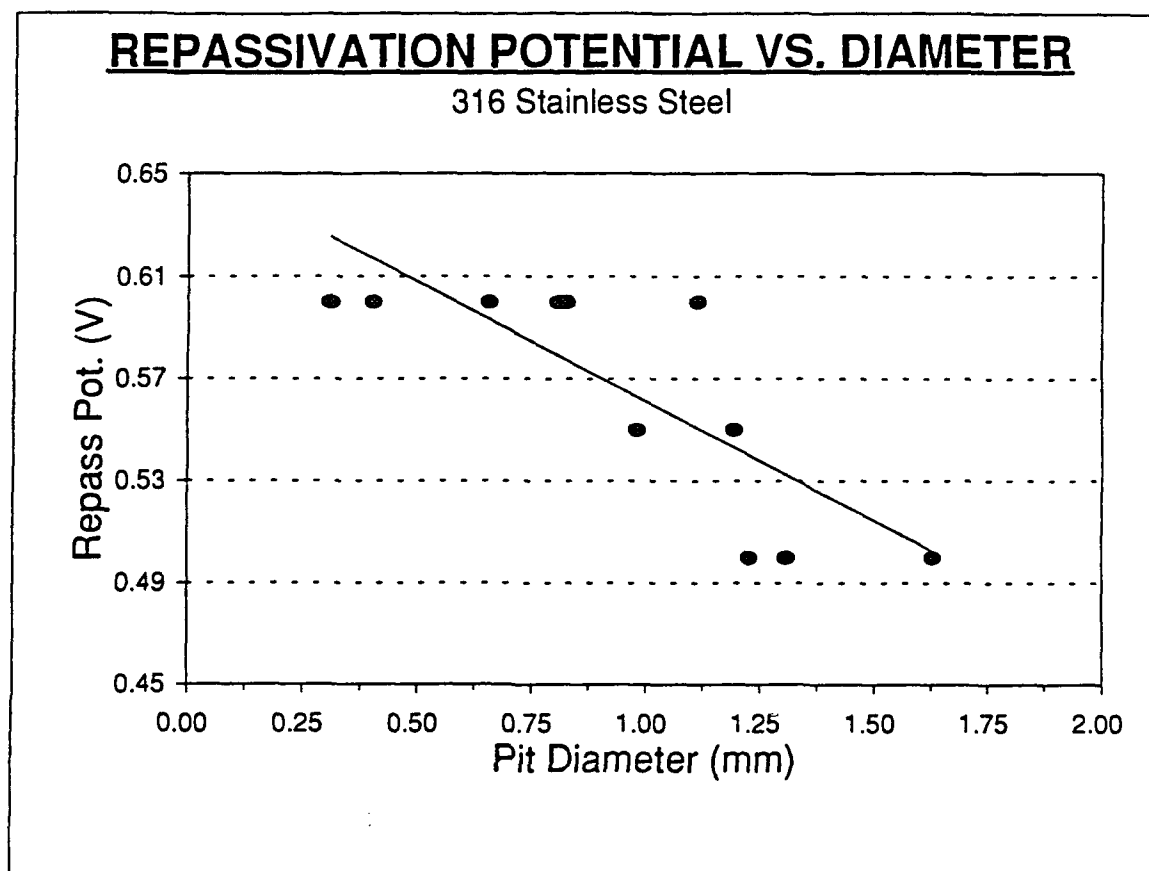
experiments, the current from the pit would stop and the SRET would no longer be able to map the site. Thus, when a pit disappeared from one map to the next, it had repassivated. In each experiment, the potential the entire specimen was being driven to by the potentiostat was known for each map. Therefore, the repassivation potential was assumed to be the potential for the first map on which the SRET failed to detect the pit. The repassivation potentials of each of the pits and their calculated physical diameter are shown in Table 4. From this data, a linear regression was calculated. The plot of the repassivation potential vs. pit diameter, shown in Figure 13, was then generated from this data.

Figure 13 clearly shows a decreasing repassivation potential with increasing pit size. The E_{rp} decreases over a range of 100 mV as the diameter of the pits increases by 1.32 mm. The slope of the linear regression indicates that, for 316 stainless steel in a simulated seawater environment, an increase of 1 mm in diameter for a pit will lower the repassivation potential of that pit by 0.093 V.

These results disagree with the data from the Newman study [2]. Newman's study only covered a range of 80 mV for the repassivation potential, and only covered a range of pit diameters of 0.25 mm compared to a range of diameters of 1.32 mm for this project. The range of pit sizes observed in this Trident Project was over five times larger

TABLE 4					
REPASSIVATION POTENTIAL VS. PHYSICAL DIAMETER FOR 316 STAINLESS STEEL					
Pit Number	Pot. (mV)	Diameter (mm)	Pit Number	Pot. (mV)	Diameter (mm)
1	0.6	0.404	7	0.6	0.829
2	0.6	0.657	8	0.55	0.983
3	0.6	0.828	9	0.55	1.19
4	0.6	1.11	10	0.5	1.31
5	0.6	0.311	11	0.5	1.63
6	0.6	0.809	12	0.5	1.23

Repassivation potentials and physical diameter (generated with calibration curve) of all 316 pits.



Regression Output:	
Constant	0.65454
Std Err of Y Est	0.02781
R Squared	0.64307
No. of Observations	12
Degrees of Freedom	10
X Coefficient(s)	-0.0933
Std Err of Coef.	0.02198

FIGURE 13: Plot of pitting potential vs. pit diameter for 316 stainless steel.

than that of Newman. Because of this greater range, the data collected in this project is more representative of the actual trend in pitting behavior than that shown in the Newman study.

One aspect of the experimental technique that could have affected the data was the rotation of the specimen while the pits corroded and repassivated. As a pit corrodes, the solution in the pit becomes more and more aggressive. The more aggressive this pit environment, the lower the potential must be dropped to cause repassivation. However, in this experiment, the specimen rotated at 100 rpm which is equivalent to a fluid velocity of roughly 0.013 m/s on the side of the specimen. Because of this fluid "flow", the solution in the pits may have been continually washed out. Thus, because of the rotation, the pit solution may not have become as aggressive as if the pit was in a quiescent environment. This may have caused the pits to repassivate at slightly higher potentials. The slight increase in the repassivation potentials due to the experimental technique would have to be taken into consideration if this system was used to determine E_{rp} for a actual cathodic protection application.

CONCLUSIONS

Based on the pitting behavior observed in the experiments presented above, the following conclusions can be drawn:

1. Although it is difficult, the relationship between repassivation potential and pit size can be determined using the SRET approach.
2. The repassivation potential for pits in AISI 316 stainless steel decreased approximately 100 mV as the pit diameter increased from .31 to 1.63 mm.
3. Calculations indicated that, for AISI 316 stainless steel in a 3.5 wt% NaCl solution, a 1 mm increase in diameter will yield a 0.093 V decrease in the repassivation potential.
4. Rotation of the specimen during pit growth and repassivation may have caused a slight upward shift in repassivation potential. Further study must be done to quantify this shift if the SRET system is to be used to generate data for cathodic protection applications. The approach used in this study could be valuable if one is interested in examining the pit size vs. E_{rp} for applications involving fluid flow. This is due to the fact that the fluid flow rate of interest can be simulated by rotating the specimen at the appropriate velocity.

5. 6061-T6 aluminum is not a suitable material for SRET scanning techniques due to its pitting characteristics.
6. If the bottom attack problem could be solved, this approach would be an excellent way of generating repassivation potential vs. pit size data for stainless steels and possibly other passive material such as titanium and nickel.

ACKNOWLEDGEMENTS

I would like to express my sincere appreciation to Professor Patrick J. Moran for his continual support and guidance throughout this project. I would like to thank William Eggers for the loan of the SRET equipment and his support of the project. I also extend my thanks to Mr. John Hein for his technical support.

REFERENCES

1. Jones, D.A., Principles and Prevention of Corrosion. Macmillan Publishing Company, New York. 1992.
2. Newman, R.C, Franz, E.M., "Growth and Repassivation of Single Corrosion Pits in Stainless Steel", Corrosion Vol. 40, No. 7, July (1941) 325-329.
3. Sridhar N., Cragolino, G.A., "Applicability of Repassivation Potential for Long-Term Prediction of Localized Corrosion of Alloy 825 and Type 316L Stainless Steel", Corrosion Vol. 49, No. 11 (1993) 885-893.
4. Thompson, N.G., Syrett, B.C., "Relationship Between Conventional Pitting and Protection Potentials and a New, Unique Pitting Potential", Corrosion Vol. 48, No. 8, August (1992) 649-659.
5. Wilde, B.E., "A Critical Appraisal of Some Popular Laboratory Electrochemical Tests for Predicting the Localized Corrosion Resistance of Stainless Alloys in Sea Water", Corrosion Vol. 28, No. 8 (1972) 283-291.
6. Moran, P.J., Natishan, P.M., "Corrosion and Corrosion Control", Kirk-Othmer Encyclopedia of Chemical Technology Fourth Ed. Vol. No. 7. New York, (1993) 548-572.
7. Szklarska-Smialowska, Z., "Pit Initiation", Advances in Localized Corrosion: Proceedings of the Second International Conference on Localized Corrosion, June 1-5, 1987, Orlando, Florida. NACE, Houston, Tex. 1990. (pp. 41-45).
8. Booklet from, "Electrochemical Techniques in Corrosion Engineering", Short Course, University of Virginia, 1991.
9. Pourbaix, M. "The Electrochemical Basis for Localized Corrosion", U.R. Evans Conference on Localized Corrosion (1971; Williamsburg Va.) NACE, Houston, Tex. 1974. (pp. 12-33).
10. Aylor, D.M., Moran, P.J., "The Influence of Incubation Time on the Passive Film Breakdown of Aluminum Alloys in Sea Water", Journal of the Electrochemical Society, Vol 133, No. 5, May (1986).

11. Metals & Alloys in the Unified Numbering System. 5th Edition, SAE & ASTM, Warrendale, PA. 1989.
12. Franz, F., Novak, P., "Effect of Rotation on the Pitting Corrosion of Aluminum Electrodes", U.R. Evans Conference on Localized Corrosion (1971: Williamsburg Va.) NACE, Houston, Tex. 1974. (pp. 576-578).